Electron signatures of active merging sites on the magnetopause

N. C. Maynard,[1,2] W. J. Burke,[3] J. D. Scudder,[4] D. M. Ober,[1] D. R. Weimer,[1] K. D. Siebert,[1] C. T. Russell,[5] M. Lester,[6] F. S. Mozer,[7] and N. Sato[8]

Received 18 June 2004; revised 20 May 2005; accepted 1 June 2005; published 13 October 2005.

[1] Near magnetopause current layers the Polar satellite often detects field-aligned fluxes of >0.5 keV electrons that carry heat flux away from merging sites along inner/outer separatrices between newly opened and closed/interplanetary magnetic flux. Close to separator lines, electron gyrotropy weakens to break trapping on closed field lines of the outer plasma sheet followed by attachment to newly opened flux at random pitch angles. Energetic electrons in the ''tails'' of distribution functions quickly move great distances along separatrices to act as surgical indicators of active merging. If IMF B_Y is large, field rotation in the magnetopause current layer can be $\ll 180^\circ$, obscuring relationships between merging sources and separatrices. Suprathermal electrons and accelerated ions moving along nearby inner and outer edges of moderate shear current layers are remote signatures of merging at widely separate locations. Detecting accelerated ions at a moderate shear magnetopause is insufficient evidence for component merging occurring near a spacecraft. During magnetopause-skimming passes Polar sampled electron tail events characteristic of inner and outer separatrices that typically lasted from a few tens of seconds to several minutes. The 557.7-nm emissions observed at cusp boundaries suggest that their sources operate on similar timescales and are active simultaneously at multiple locations. The magnetic conjugacy of inner separatrices with cusp boundaries as well as the similar timescales of electron tail and 557.7-nm emission events strongly indicates that they are causally connected. Combining the two types of measurements offers an effective technique for separating temporal and spatial variability in magnetopause dynamics.

Citation: Maynard, N. C., W. J. Burke, J. D. Scudder, D. M. Ober, D. R. Weimer, K. D. Siebert, C. T. Russell, M. Lester, F. S. Mozer, and N. Sato (2005), Electron signatures of active merging sites on the magnetopause, *J. Geophys. Res.*, *110*, A10207, doi:10.1029/2004JA010639.

1. Introduction

[2] Critical interactions between interplanetary plasma and the magnetosphere occur along the dayside magnetopause. The kinds and intensities of the interactions depend largely on the degree of magnetic shear found at the interface between the interplanetary magnetic field (IMF) and the Earth's field. In regions of high shear (nearly antiparallel) magnetic merging dominates [*Crooker*, 1979]. In regions of low shear (nearly parallel) the transport of magnetic flux is impeded, and plasma is squeezed out of IMF flux tubes to form depletion layers [*Zwan and Wolf*, 1976]. Many features of magnetospheric interactions with the magnetosheath plasmas and magnetic fields are now empirically established. However, properly instrumented spacecraft seldom venture for long periods into regions of active magnetic merging. Even then, they only provide measurements at single locations and instants of time. Thus our understanding of the large-scale spatial and temporal merging structures is limited. Detailed analyses of remotely sensed merging signatures are useful for understanding the large-scale aspects of magnetopause interactions and their consequences in the high-latitude ionosphere.

[3] Maynard and coworkers showed that enhanced 557.7 nm emissions near the dayside cusp occur in detailed concert with changes in the IMF [*Maynard et al.*, 2001c, 2004b; *Maynard*, 2003, 2005]. Their empirical results suggest that all-sky images of 557.7 nm emissions act as ''television'' pictures of merging on the conjugate magnetopause. *Maynard et al.* [2004b] analyzed energetic electron measurements acquired during a DMSP F-15 overflight of a dayside auroral form that was active above

[1]ATK Mission Research, Nashua, New Hampshire, USA.
[2]Now at Space Science Center, University of New Hampshire, Durham, New Hampshire, USA.
[3]Air Force Research Laboratory, Hanscom Air Force Base, Massachusetts, USA.
[4]Department of Physics and Astronomy, University of Iowa, Iowa City, Iowa, USA.
[5]Institute of Geophysics and Planetary Physics, University of California, Los Angeles, California, USA.
[6]Department of Physics and Astronomy, University of Leicester, Leicester, UK.
[7]Space Sciences Laboratory, University of California, Berkeley, California, USA.
[8]National Institute of Polar Research, Tokyo, Japan.

0148-0227/05/2004JA010639$09.00

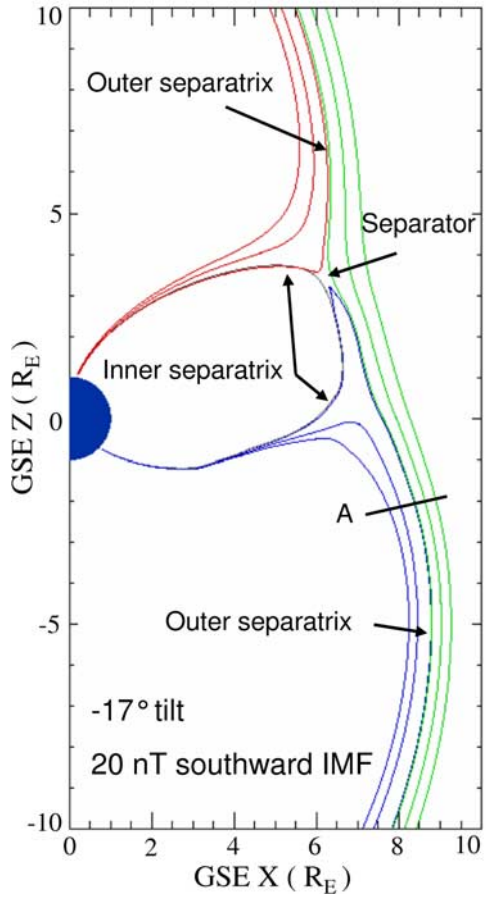

Figure 1. Magnetic field line configuration derived from a MHD simulation using the ISM code with IMF input of a 20 nT southward and a $-17°$ dipole tilt. Blue (red) field lines are open from the Northern (Southern) Hemisphere. Green field lines connect to the IMF on both ends. As a result of the dipole tilt, the merging site is located near the rim of the cusp in the hemisphere away from the tilt. Line A represents a crossing through the magnetopause in the simulation that is analogous to the Polar data from 31 March 2001 (see text).

Svalbard and nonsimultaneous Polar observations of merging to argue that suprathermal (0.5–2 keV) electrons propagating away from active merging sites are the sources of the 557.7 nm emissions. This paper seeks to confirm the conjectured physical connection between electrons emerging from active merging sites and 557.7 nm emissions near dayside cusp boundaries. We do this through close examinations of field-aligned suprathermal electron beams, or ''tails'', that the Polar satellite observed episodically during two orbits along the dayside magnetopause in March 2001. The proximity of this electron population to field-aligned ion and Alfvénic Poynting fluxes indicates that they are indeed magnetically conjugate to active merging sites [*Maynard et al.*, 2003]. During both orbits the interplanetary magnetic field (IMF) B_Z was southward. In the second case the magnitude of IMF B_Y was significant.

[4] We use predictions of a two-dimensional (2-D) model of merging proposed by *Gosling et al.* [1990] to help interpret Polar electron observations during the IMF-B_Z dominant case. It is necessary to extend the model to three dimensions to understand situations when IMF B_Y is large. Magnetosheath and plasma sheet particles entering the merging separator region become demagnetized [*Cowley*, 1982; *Scudder et al.*, 2002] and mix before being ejected along inner and outer separatrix field lines. Figure 1 is a schematic adaptation of the *Gosling et al.* [1990] model to circumstances appropriate for the Polar orbit of 31 March 2001. Magnetic field lines traced by the Integrated Space Model (ISM) [*White et al.*, 2001] transition from purely IMF (green) to open with one end tied to the ionosphere via the northern (red) and southern (blue) cusps. The black line corresponds to the last closed field line. The boundaries between closed field lines and open field lines mark inner separatrices. The transitions from open to IMF field lines correspond to outer separatrices. Because of their high speeds (>15,000 km/s), energetic electrons remain closer to separatrix field lines than slower moving accelerated ions. The model predicts that during periods of southward IMF, Polar should observe electrons moving away from merging sites along outer separatrices sunward of ion streams. Conversely, electron beams near inner separatrices are located earthward of ion flows. Because inner separatrix electrons quickly mirror off the ionosphere, observed fluxes should be bidirectional. During periods of significant B_Y, the usefulness of a 2-D representation of the magnetopause current layer diminishes. We defer our description of the 3-D extension of the model. The chief difference between the two models is that spatially close inner and outer separatrix field lines connect to widely separated merging sites in the magnetopause current layer.

[5] *Sonnerup et al.* [1981] and *Scudder et al.* [1984] reported measurements of electron heat fluxes propagating away from merging separators. Heat flux calculations emphasize asymmetries in the highest energies of a population. Others have focused on the low-energy portions of electron distributions. *Fuselier et al.* [1995, 1997] interpreted AMPTE-CCE observations of field-aligned electrons with $E < 770$ eV at low-magnetic shear magnetopauses as having originated in the magnetosheath. Electrons with $E \approx 1$ keV most likely came from the magnetosphere. Counterstreaming electrons at these energies detected in the magnetopause current layer were regarded as resulting from AMPTE being between magnetosheath sources and ionospheric mirrors. This contrasts with the earlier conclusion of *Ogilvie et al.* [1984] that bidirectional fluxes indicate closed local field lines. Because of bidirectional streaming, *Fuselier et al.* [1997] concluded that bidirectional streaming electrons were not useful for determining the open-closed topology of field lines in the low-latitude boundary layer. On the magnetosheath side of the magnetopause current layer AMPTE encountered unidirectional streaming electrons. They argued that streaming electrons and accelerated ions indicate that merging was occurring at subcusp latitudes in regions of low magnetic shear. *Onsager et al.* [2001] suggested that shifts in average electron energies could be used to discriminate between local and distant dayside merging sites.

[6] On the other hand, our analysis assumes that a population trapped in the outer plasma sheet constitutes the original reservoir for most energetic electrons that

reach the ionosphere to excite 557.7 nm emissions. The initial redirection of the trapped electrons to field-aligned streaming populations occurs after demagnetization and nonguiding center motion within the diffusion region. Further acceleration may occur during the merging process and/or near the ionosphere. In the absence of reflection from the bow shock, field-aligned electron fluxes near the outer separatrix only move away from the separator. Because high-speed electrons move quickly to exit the diffusion region and subsequently remain tightly bound to magnetic field lines, we expect to observe electron beams only while merging is actively occurring.

[7] The following sections provide brief descriptions of our measurement techniques and the ISM magnetohydrodynamic (MHD) model used to interpret Polar observations during encounters with inner and outer separatrices. Expectations based on ISM simulations with a significant B_Y provides a semiquantitative framework for interpreting an event on 12 March 2001. In this example of moderate ($\sim$90°) shear at the local magnetopause, electron tails were observed on both sides of the current layer. ISM results indicate that they came from different separator (merging) regions. Section 5 (1) establishes the remote, nonlocal source of the tail electrons, (2) compares properties of the field-aligned electron beams to those of the 557.7 nm cusp emissions, and (3) comments of the 3-D structure of the magnetopause.

2. Measurement Techniques

[8] The Advance Composition Explorer (ACE) spacecraft provided critical background information while measuring interplanetary conditions near the L_1 point, $\sim$234 R_E upstream of Earth. The Solar Wind Electron, Proton, and Alpha Monitor (SWEPAM) measured the solar wind velocity and density [*McComas et al.*, 1998]. A triaxial fluxgate magnetometer measured the three components of the interplanetary magnetic field (IMF) vector [*Smith et al.*, 1998].

[9] Polar's apogee (9 R_E) was near the equator in 2001, and for long intervals in March the orbit skimmed from south to north along the dayside magnetopause. From this vantage Polar could monitor magnetopause responses to temporal changes of the IMF and solar wind plasma. This study primarily uses data from three sensors on Polar.

[10] 1. The Hydra Duo Deca Ion Electron Spectrometer (DDIES) consists of six pairs of electrostatic analyzers looking in different directions to acquire high-resolution energy spectra and pitch angle information [*Scudder et al.*, 1995]. Distributions of electrons with energies between 1 eV and 10 keV and ions with energies per charge ratio of 10 eV q^{-1} to 10 keV q^{-1} are provided every 2.3 s.

[11] 2. The electric field instrument (EFI) uses a biased double probe technique to measure vector electric fields from potential differences between three orthogonal pairs of spherical sensors [*Harvey et al.*, 1995]. This paper uses measurements from the long wire antennas in the satellite's spin plane.

[12] 3. The Magnetic Field Experiment (MFE) consists of two orthogonal triaxial fluxgate magnetometers mounted on nonconducting booms [*Russell et al.*, 1995].

[13] EFI and MFE sampling rates were 40 and 20 s^{-1}, respectively. Data presented here are spin averaged using least squares fits to sine functions.

3. Integrated Space Weather Prediction Model

[14] ISM uses standard MHD equations augmented by hydrodynamic equations in the collisionally coupled thermosphere. It operates within a warped cylindrical computational grid, that extends 40 R_E sunward, and 300 R_E antisunward from the origin at the center of the Earth, and 60 R_E radially from the Earth-Sun line. The cylindrical grid has an interior spherical boundary approximately located at the bottom of the E layer (100 km). The cylindrical to spherical interface (near 3.5 R_E) warps from purely spherical at 3.5 R_E to purely cylindrical at large distances [*White et al.*, 2001]. Approaching the Earth, equations are solved in a seamless manner from pure MHD in the Solar Wind to those appropriate for the low-altitude ionosphere/thermosphere.

[15] Simulation results discussed here were obtained with specifically selected parameters and simplifying approximations. The spatial resolution of ISM's finite differences varies from a few hundred kilometers in the ionosphere to several R_E near the outer boundary of the computation domain; it ranges from 0.2 to 0.8 R_E at the magnetopause. Explicit viscosity in the plasma momentum equation was set to zero. In solving the Ohm's Law equation the explicit resistivity coefficient was set to $\nu = 0$ if current density normal to **B** is $j_\perp < 3.16 \times 10^{-3}$ A m^{-2}. In regions with $j_\perp$ above this threshold, $\nu = 2 \times 10^{10}$ m^2 s^{-1}. In practice, this choice leads to nonzero explicit resistivity near the subsolar magnetopause, and in the nightside plasma sheet. Where needed to maintain numerical stability, dissipation is based on the partial donor cell method (PDM) as formulated by *Hain* [1987]. Dissipation is necessary in the code to approximate nonlinear magnetic reconnection.

4. Observations

[16] During the magnetic superstorm of 31 March 2001, the subsolar magnetopause was compressed earthward of geosynchronous altitude, and thus well inside Polar's apogee, for a large portion of the day [*Ober et al.*, 2002]. Polar crossed the magnetopause outbound, poleward of the Southern Hemisphere cusp near 0600 UT. The IMF was predominantly southward. Near 0600 UT the north dipole axis tilts antisunward about −12°. Figure 1 provides a schematic context for visualizing the geophysical background for Polar measurements. The traced magnetic field lines derive from an ISM simulation with a 20 nT southward IMF and a dipole tilt of −17°. The line marked, by the symbol A, indicates the approximate places where Polar encountered the magnetopause on 31 March 2001. Located poleward of the cusp, Polar could only cross outer separatrices. Temporal IMF and solar wind pressure variations allow the slowly moving Polar to move back and forth across separatrices multiple times during a given orbit.

4.1. The 31 March 2001 Event

[17] Polar entered the magnetosheath poleward of the Southern Hemisphere cusp on 31 March 2001, when the

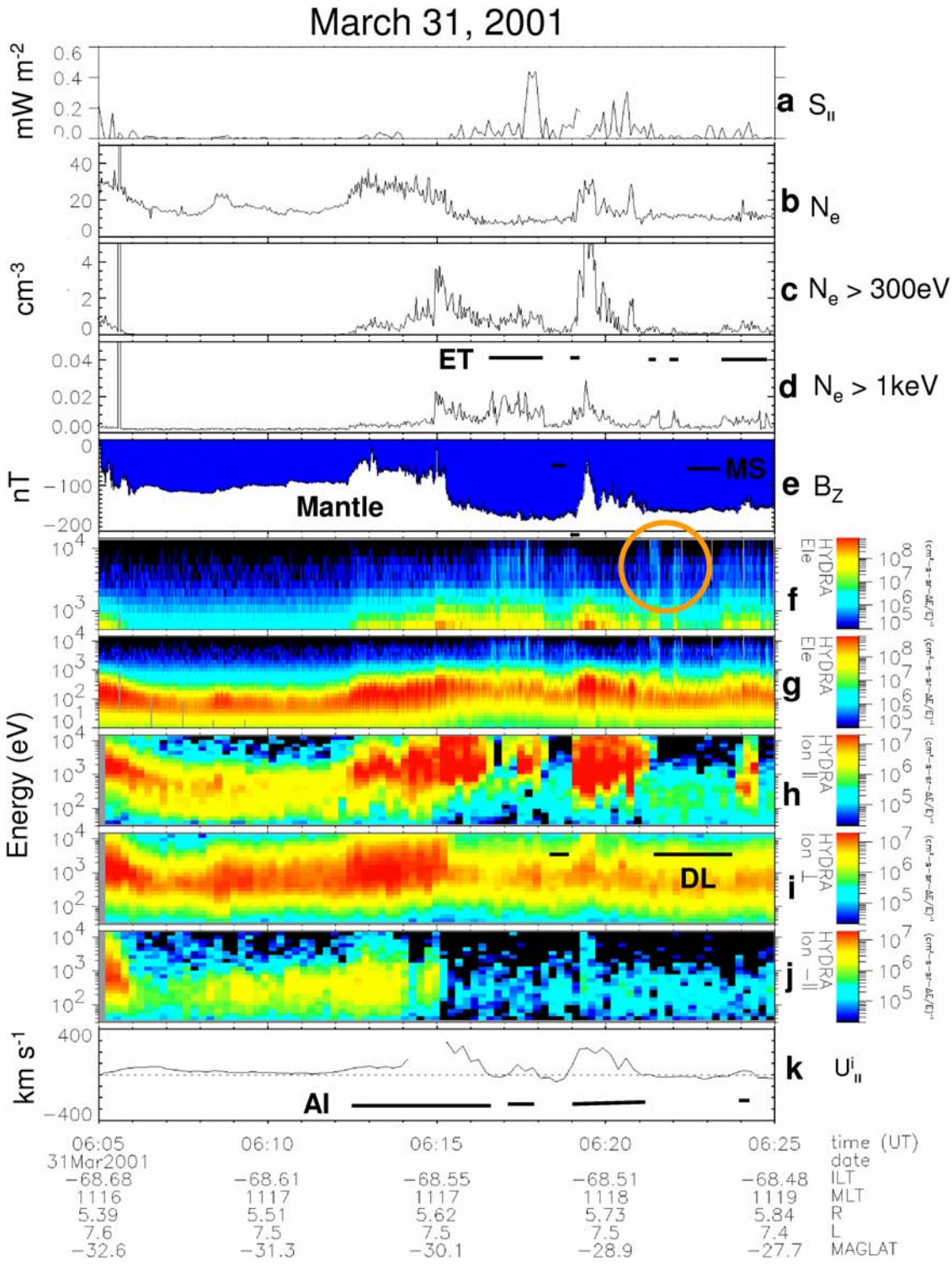

Figure 2. Polar data for the outbound (Southern Hemisphere) separatrix crossing on 31 March 2001, showing (a) parallel Poynting flux, (b) the super thermal electron density, (c) electrons above 300 eV, (d) electrons above 1 keV, (e) the Z component of the magnetic field, (f) electron energy spectra above 500 eV, (g) the total measured electron energy spectra, (h) parallel ion energy spectra, (i) perpendicular ion energy spectra, (j) antiparallel ion energy spectra, and (k) the parallel ion velocity. Regions of entry onto magnetosheath field lines are noted by the black bars in Figure 2e. The magnitude of B_Z is enhanced in the magnetosheath and on the first open field lines where accelerated ions are seen and enhanced parallel ion velocity are seen (noted by the bars in Figure 2k). The enhanced magnetic field is a signature of depletion areas. Electron tails are marked by the black bars in Figure d. The electron tail detailed in Figure 3 is highlighted by the orange circle.

IMF magnitude was 45 nT and the clock angle 160°. At the time the south magnetic pole tilted 17° toward the Sun. Measurements acquired between 0605 and 0625 UT are displayed in Figure 2. Figure 2a shows the component of wave Poynting flux parallel to the average, local magnetic field. Figures 2b, 2c, and 2d show the total electron density, the integrated density above 300 eV, and the integrated density above 1 keV, respectively. The B_Z component measured by MFE is shown in Figure 2e. Figures 2f and 2g present the spectra of electrons with $E > 500$ eV and over the whole energy range, respectively. Ion fluxes measured in the parallel (Figure 2h), perpendicular (Figure 2i) and antiparallel (Figure 2j) directions are displayed in the bottom three spectrograms. The component of ion drift velocity parallel to local **B** is shown in Figure 2l. A similar format for data display formats is followed in Figures 5 and 7 in section 4.2.

[18] Markings on Figure 2 help locate data relative to magnetospheric boundaries. The mantle and magnetosheath (MS) are noted in Figure 2e. Poleward of the Southern Hemisphere cusp IMF B_Z and adjacent open field lines in the magnetosphere have the same polarity. Thus no field-reversal occurred at the magnetopause. As illustrated in Figure 2 of *Siscoe et al.* [2004], under the extreme conditions of the 31 March 2001 superstorm the cusps moved equatorward and the shape of the magnetopause developed shoulder-like features poleward of them. Depletion layers formed in front of these shoulders where plasma flow is locally impeded until the IMF field lines drape to merging sites [cf. *Maynard et al.*, 2004a, Figure 9]. Depletion layers are noted by the dashed lines labeled DL and are characterized by intensifications of B_Z, decreased plasma densities, and mainly perpendicular ion fluxes (Figure 2i). Polar detected three strong accelerated ion (AI) events in regions of enhanced B_Z (Figure 2h). AI events, denoted by a dashed line, are associated with significant parallel ion velocities, indicating that the events occurred on newly opened field lines (Figure 2k). Bursts of enhanced keV electron tails (ET) evident in Figure 2f, are labeled by a dashed line in Figure 2d. In highlighted ET intervals, the fractional change in the keV electron density was larger than that of the total number density (Figure 2b). IMF field lines of the magnetosheath (MS) are highlighted by the two dashed lines in Figure 2f which highlight regions between the electron tails with no accelerated ions and depleted plasma. The depletion layers noted in Figure 2i, encompass the excursions into the magnetosheath as well as regions of just merged field lines marked by the electron tails.

[19] Attention is directed to enhanced ion (Figure 2h) and wave Poynting flux (Figure 2a) parallel to **B** detected just prior to 0621 UT. The combined presence of these remote signatures are necessary but are not sufficient conditions for identifying actively ongoing merging [*Maynard et al.*, 2003]. As highlighted by the orange circle, the flux of electrons with $E > 1$ keV increased (Figure 2f) just after 0621 UT at the outer edge of the enhanced ion velocity (Figure 2l) and accelerated parallel ions (Figure 2h). This high-energy tail is seen in the electron spectrograms (Figures 2f and 2g) and in the integrated density >1 keV (Figure 2d). Consistent with predictions of *Gosling et al.* [1990] the keV tail on electron distributions is a product of merging that should be, and in fact was, detected closer to the separatrix than ions that were simultaneously accelerated during the merging event.

[20] Figure 3 shows plots of four electron and ion distribution functions measured during the 0621 UT outbound crossing of the outer separatrix. The velocity distributions of electrons and ions were averaged over gyrophase angles and are displayed as functions of the velocity components parallel and perpendicular to **B**. The velocity space axis along **B** points to the right. To produce these pictures Hydra measurements from all sampled pitch angles were rotated into a common plane assuming gyrotropy. The curves in the upper half plane are the result of this folding. By averaging and redistributing them in the lower half plane, we implemented true gyrophase averages. The bottom halves of samples were computed assuming symmetry about **B**. The faint white lines indicate the minimum pitch angles observed during a selected interval as functions of particle energy. Ion displays give true pitch angle distributions, having been shifted by their measured perpendicular drift velocities into the comoving frame of reference.

[21] Figures 3e and 3f show distributions of ions accelerated along **B**. In addition to accelerated magnetosheath ions, the data show an intense core of accelerated magnetospheric ions with parallel velocities of 400 km s^{-1}. The pancake-shaped ion distribution in Figure 3h is typical of depletion layers near the magnetopause. Only high-energy electrons moving along **B** (Figure 3d) accompany pancake magnetosheath ions within the depletion layer (Figure 3h). They correspond to the electron tail highlighted in Figure 2f, and appeared after the last vestige of accelerated ions (Figure 3g) vanished. Low-energy electron contours are asymmetric, shifted toward the parallel direction. Nearly isotropic electron distributions were seen during intervals of field-aligned ion fluxes (Figures 3a and 3b).

[22] We note that Figure 2 also shows that Polar sampled even higher concentrations of keV electrons beams just after 0619 UT. In this case, distribution function plots (not shown) indicate that the electrons were encountered earlier in time than ions as the spacecraft reentered the ion acceleration region and before its later outbound exit at 0621 UT. Other regions of enhanced keV electrons are seen near 0617 and 0624 UT, highlighted by the dashed lines in Figure 2d. These are again near the boundaries of accelerated ions. Signatures of merging continue to be seen in these regions of accelerated ions and wave Poynting flux parallel to **B**.

[23] The Polar measurements of 31 March confirm the *Gosling et al.* [1990] model, showing that it is conceptually valid for IMF clock angles near 180°. high-energy electron beams directed away from the merging site defined the electron boundary. Electron boundaries were closer to separatrices than the ion boundaries. Field-aligned flows were directed away from the source at outer separatrices. Electron tails complement earlier identifications of separatrices from measurement of heat flux [*Scudder et al.*, 1984], and they provide remote diagnostics for active merging, even when the detecting satellite is poleward of the cusp.

4.2. The 12 March 2001 Event

[24] When the magnitude of IMF B_Y is significant, the complexity of merging geometries increases. Between 1600 and 1700 UT on 12 March 2001, Polar experienced a series

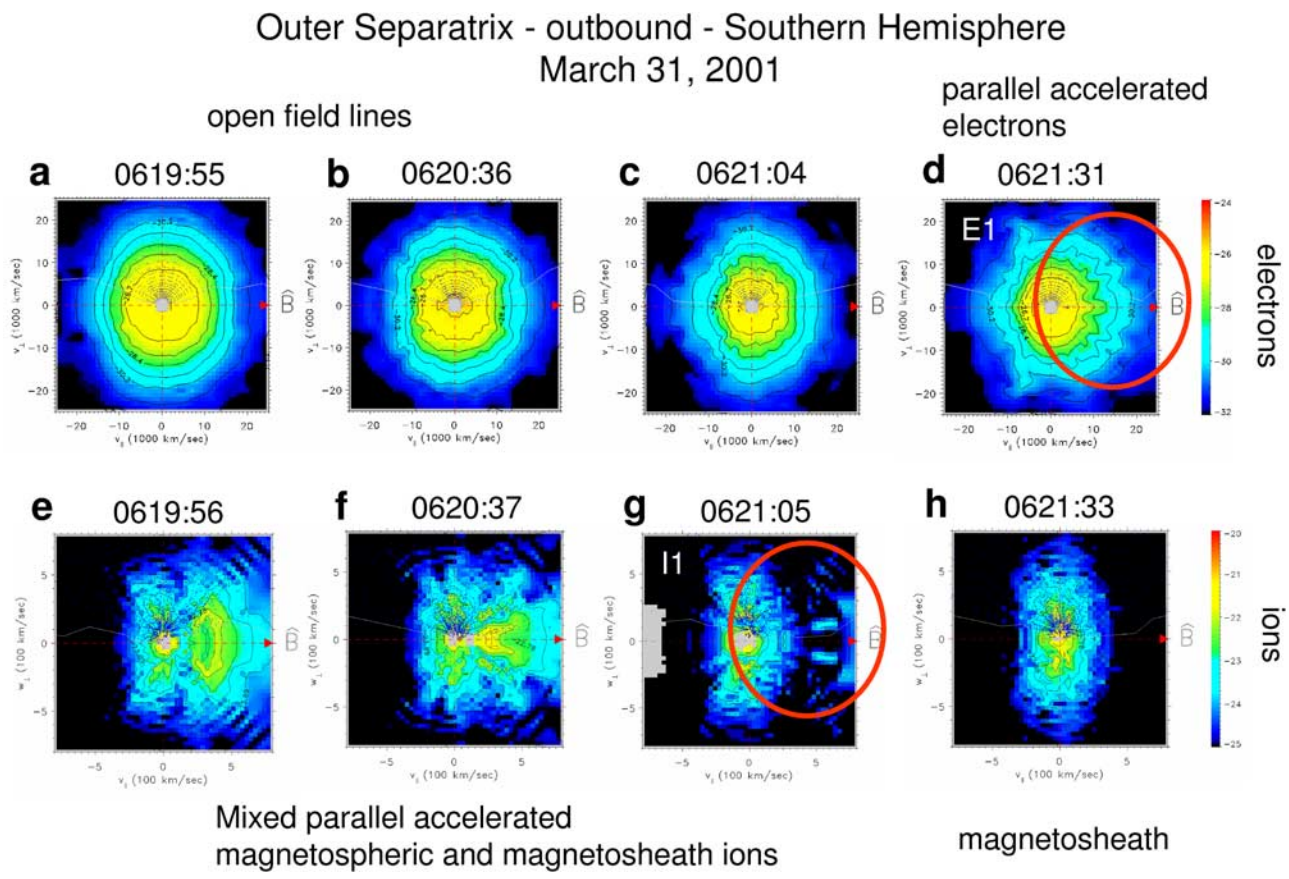

Figure 3. Electron and ion velocity distribution plots for the outbound crossing of the outer separatrix from open to magnetosheath field lines on 31 March 2001. The top half of the distribution function is measured, while the bottom half is created by symmetry. The faint white line defines how close to *B* measurements are made for that particular distribution function. The electron and ion boundaries are noted by E1 and I1. The ion distributions have been shifted by the perpendicular ion velocity to place them in the frame moving with the plasma.

of magnetopause crossings near 50° north magnetic latitude and 1330 MLT. The IMF had a significant $B_Y < 0$ component. During this UT interval the magnetic dipole axis tilted toward the Sun. The principal antiparallel merging sites should be at prenoon and postnoon locations in the Northern and Southern hemispheres, respectively [*Maynard et al.*, 2003]. Thus Polar's trajectory should map to the convection cell tied to a distant merging sites in the Southern Hemisphere.

[25] Before examining Polar measurements it is useful to consider an ISM simulation of dayside magnetopause interactions under analogous geophysical circumstances, with the dipole axis tilting 17° sunward and an IMF of 5 nT at a clock angle of −135°. Figure 4 shows a 3-D representation of the surface of last closed magnetopause field lines, color-coded by log $|B|$. ISM traces magnetic field lines from the high-latitude ionosphere to the conjugate hemisphere. The tracer algorithm identifies the latitude at each local time where field lines transition from open to closed. The locus of transition points defines the surface last closed field lines shown in Figure 4. Green and black areas on this surface mark regions of weak magnetic fields, and act as proxies for locations of merging occurrence. The vertical line represents the X-Z plane intersecting the magnetopause at the location of Polar. At ionospheric footprints of "last closed field lines", the algorithm steps 1 km poleward to trace nearby "first open field lines." Traces of several first open field lines are superimposed over the magnetopause surface.

[26] Magnetopause currents tilt the orientation of the closed field lines near the boundary. Streaks on the surface that cant northward from postnoon to prenoon illustrate the tilt of the last closed field lines (see red arrows). To establish the locations of merging sites applicable to the vicinity of Polar's trajectory, consider the first open field line emerging from the northern ionosphere, colored blue and marked by the symbol (s). Near 1330 MLT field line (s) enters the magnetopause current layer as an inner separatrix. Outside the current layer it initially follows nearby closed field lines that tilt toward the southeast then hooks northward and toward dusk as an outer separatrix. The corresponding first open field line emerging from the southern ionosphere, colored red and marked by the symbol (r), hooks back toward dawn as an outer separatrix. The orange circle highlights the approximate applicable merging separator's location. An IMF field line (q) in the adjacent magnetosheath is colored green.

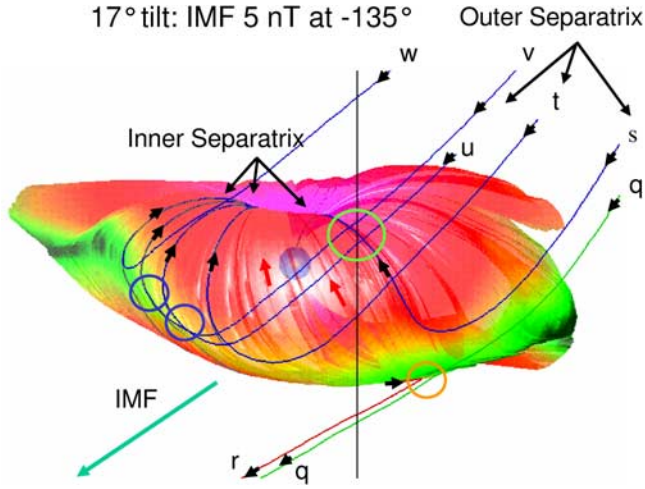

Figure 4. A 3-D view of the magnetopause from a MHD simulation with a 17° dipole tilt and IMF conditions of 5 nT at a clock angle of −135° (negative B_Y). The image was created by painting the last closed field line surface with the log of the magnetic field magnitude. The closed field lines at the nose are canted from postnoon to prenoon (highlighted by the red arrows). Selected first open field lines r and s near 1330 MLT are shown along with a nearby magnetosheath field line q. The probable merging location is highlighted by the orange circle. Four other first open field lines ((t, u, v, and w) traced from the prenoon northern ionosphere are also shown. Their probable merging sites are indicated by the blue circles. The open field lines have arrow heads corresponding to the direction of the magnetic field. Where the outer portions of u and v are draped across the inner part of s is highlighted by the green circle. This is the approximate location of Polar in the 12 March event presented in Figures 5–9.

[27] Four first open field lines (t, u, v, and w) connect to prenoon merging sites and drape over the subsolar magnetopause. Two of these open field lines (u) and (v) cross the first open field line (s) at nearly right angles near the location of Polar (green circle). Blue circles mark the approximate locations of their merging separators. After bending backward from the prenoon merging sites they drape over the magnetopause close to the outer edge of the current layer. They are thus representative of outer separatrix field lines. Near the location of Polar, recently opened field lines on the magnetosheath side of the magnetopause may connect to very different merging sites than the nearby inner separatrix field line (s) on the magnetospheric side of the current layer.

[28] Within the green circle, the rotation angle is nearer 90° than 180° across the magnetopause current layer. As the magnetic field in this example rotates in the current layer, the Y component remains nearly continuous while the Z component reverses polarity. Thus the magnetic field orientation provides a discriminator as to which separatrix and conjugate merging site is being sampled. Although merging signatures can be seen on either side of this moderate shear magnetopause current layer, they come from different, well-separated source locations. Both projected source locations are remote from Polar. Simple 2-D pictures of merging geometry, exemplified by *Gosling et al.* [1990] and our Figure 1, fail to capture the 3-D complexity added by IMF B_Y.

[29] To illustrate and expand on these points, we consider three intervals on 12 March 2001, when Polar entered the magnetopause current layer. Because its orbit tended to skim along the magnetopause, in most encounters Polar did not fully cross the current layers. The first example, involves an inner separatrix crossing near 1625 UT while Polar was at high magnetic latitudes. With the addition of local B_Y (Figure 5f), Figure 5 presents Polar data acquired from 1610 to 1640 UT in the same format as Figure 2. Between 1619 and 1624 UT Polar was clearly in the magnetosphere where it sampled low-density plasmas (Figure 5b). After a brief excursion into the boundary layer, the region of low density continued until 1625 UT. At this time an electron tail is seen (orange circle) that was quickly followed by accelerated parallel ions and enhanced parallel ion velocity. The direction of ion flow indicates that the source region was equatorward of the spacecraft. Multiple B_Z reversals are accompanied by accelerated ions and wave Poynting flux. High-energy electron tails appear and disappear quickly at these high, subcusp latitudes as the spacecraft moves into and out of the current layer. While the observed variations clearly involve spatial changes, they may also have temporal contributions.

[30] Figure 6 gives an expanded view of the inner separatrix crossing at 0625 UT. Figure 6a shows the Z_{GSM} magnetic field component measured at Polar's location during the entire 1610 to 1640 interval. Fluxes of electrons parallel and antiparallel to **B** are presented in Figures 6l and 6m, respectively. Five electron and ion distribution functions compiled near the separatrix crossing appear in Figures 6b through 6k. In this case Polar was skimming the magnetopause equatorward of the northern cusp near 1330 MLT. Red lines key times when the distribution functions were acquired. The sequence begins just inside the magnetopause where, plasma sheet electrons (Figure 6b) have trapped distributions and the ions (Figure 6g) are cold and isotropic. Accelerated magnetosheath ion fluxes (Figures 6i and 6j) peaking along **B** come from sources equatorward of the spacecraft. Prevailing negative IMF B_Y and B_Z conditions indicate an afternoon antiparallel merging site in the Southern Hemisphere [cf. *Maynard et al.*, 2003, 2004b]. The distribution functions of high-energy electrons, highlighted by the red circle in Figure 5i, are represented in Figures 6c and 6d. They reached Polar ahead of the enhanced ion fluxes. Because of their high speeds and proximity to the northern ionosphere, both incident and reflected high-energy electron fluxes were detected. Note that electron fluxes perpendicular to **B** have higher energies than those of the adjacent plasma sheet. For comparison, the electron and ion distribution functions in Figures 6f and 6k are characteristic of magnetosheath particles at the current layer's outer edge. Data in Figure 6 establish that electron distribution functions near the inner separatrix had bidirectional high-energy tails and were connected to a merging site equatorward of the spacecraft.

[31] In the half hour after 1640 UT Polar detected multiple, unidirectional (antiparallel) electron tail events.

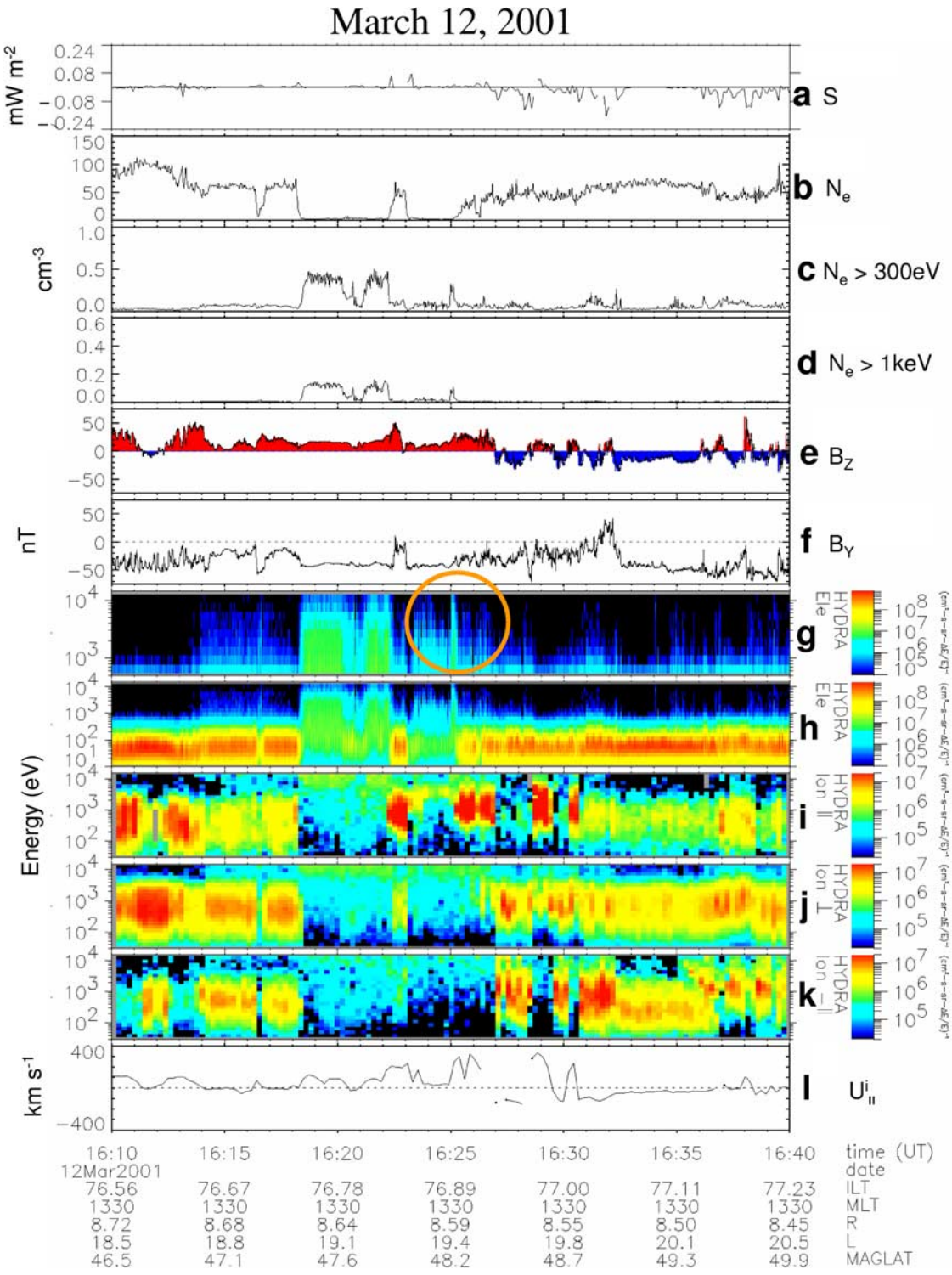

Figure 5. Polar data for the interval from 1610 to 1640 UT on 12 March 2001, in the format of Figure 2. Note that the measured B_Y is included (Figure 5f), and the spectrograms have been shifted down by one letter. The orange circle notes the region of the electron tail highlighted by Figure 6.

Figure 7 shows data from this period in the same format as Figures 2 and 5. Throughout the interval Polar was mostly in either the magnetosheath or the magnetosheath side of the current layer. The electron spectrogram contains sporadic bursts of high-energy electron tails antiparallel to **B**. Accelerated antiparallel ion fluxes appear and disappear at relatively discreet energies, in coincidence with small antiparallel bulk velocity enhancements (Figure 7l). Brief

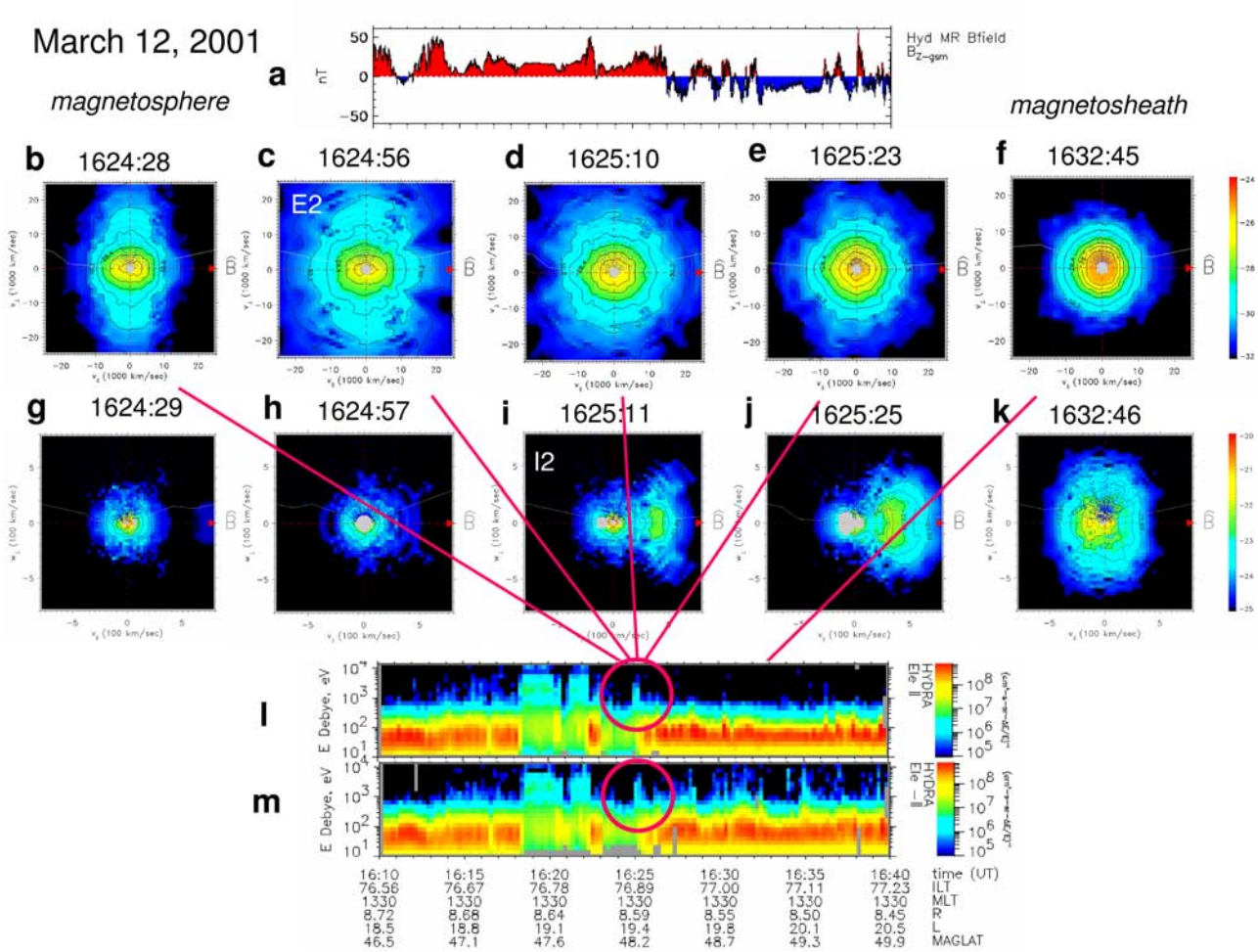

Figure 6. Outbound crossing of the inner separatrix on 12 March 2001. (a) Z component of the magnetic field displaying on which side of the magnetopause current layer the satellite is located: red (blue) for magnetosphere (magnetosheath); (b–k) electron and ion velocity distribution functions; (l–m) parallel and antiparallel electron energy spectrograms. The IMF clock angle at this time was approximately −135°. See also caption for Figure 3.

excursions into the center of the current layer, indicated by reversals in the polarity of B_Z, are highlighted by vertical lines. During each excursion antiparallel ion fluxes were detected near the highest energies. Data shown in Figure 8 allow detailed investigations of the two intervals marked by circles in Figure 7g.

[32] Figure 8 presents measurements taken by between 1640 and 1710 UT of B_Z (Figure 8a), electron distribution functions (Figures 8b–8k) as well as the antiparallel fluxes of ions (Figure 8l) and electrons (Figure 8m). Selected electron and ion distribution functions highlight electron tail events, keyed by the lines to the spectrogram of Figure 8m. B_Z was primarily southward indicating that Polar was mainly in the outer part of the magnetopause current layer (Figure 5). Between 1642 and 1644 UT, electron tails appeared almost continuously in the spectrogram. Antiparallel high-energy electrons are clearly seen in the distribution functions (Figures 8b–8e). The accelerated fluxes all came from equatorward of the spacecraft during this encounter with an outer separatrix. Throughout this long sequence of high-energy electron fluxes (Figure 8m) there is little evidence of ion acceleration until 1643:21 UT (Figure 8f), as highlighted by the first vertical black line.

[33] A second encounter with an outer separatrix occurred near 1657 UT when Polar detected antiparallel ions and electron tails. Apparently Polar moved from the center of the current layer toward the magnetosheath then back toward the center. Electron distributions in Figures 8h–8k consistently showed antiparallel, high-energy tails. Polar observed the most intense fluxes of high-energy electrons (Figures 8i and 8j) at the outer edge of the current layer as indicated by a negative spike in B_Z. At 1657 UT the spacecraft was in the middle of the current layer where $B_Z \approx 0$. The second vertical line marks the location of the highest antiparallel ion fluxes (Figure 8g), that were detected before the strong electron tail fluxes. Again, time sequences of antiparallel ion fluxes seem to alternate between several discreet energies. This suggests a discontinuous process leading to a temporal dispersion signature.

[34] A comparison of the ion and electron spectrograms in Figures 8l and 8m suggests a rather complex picture.

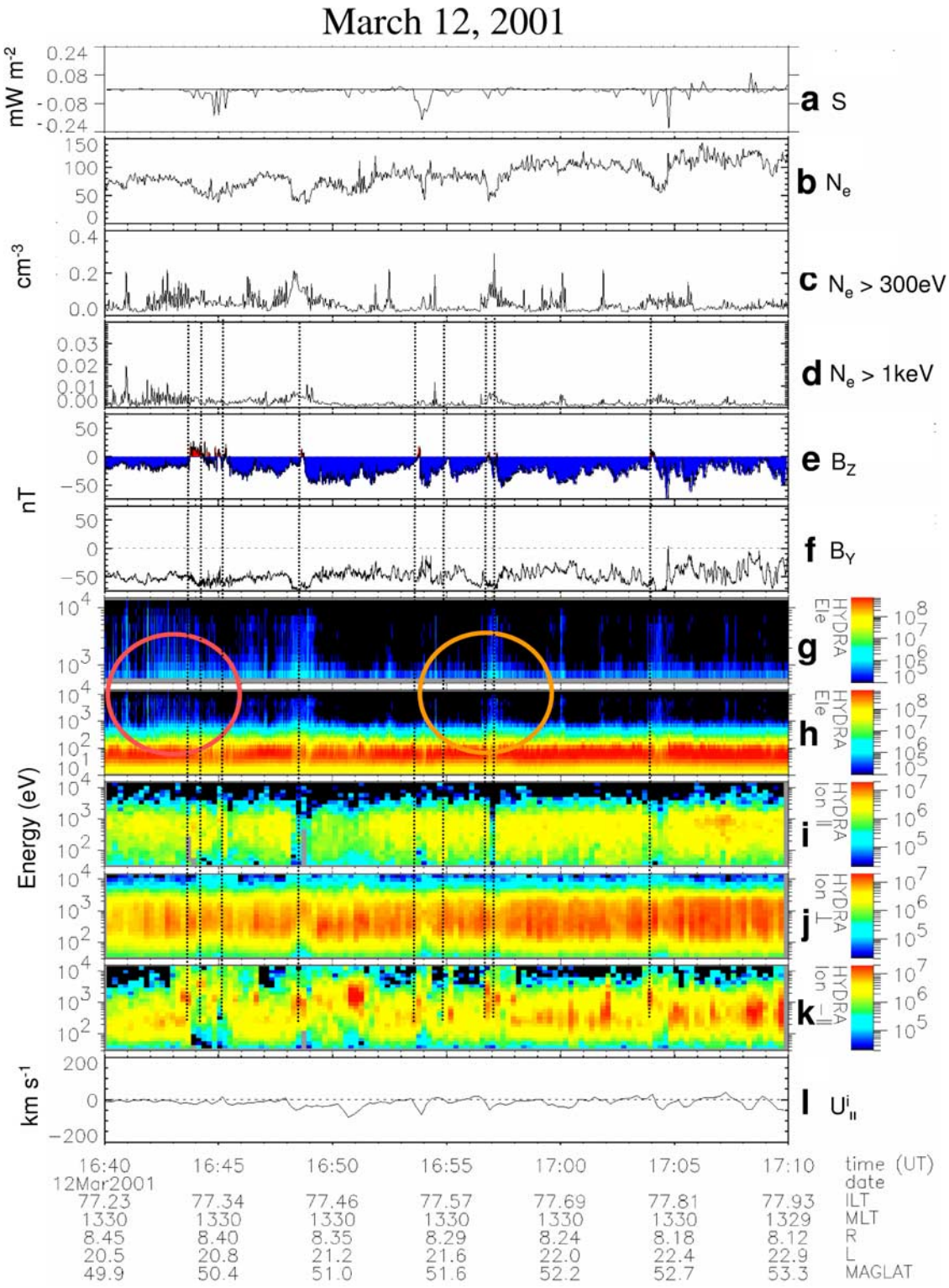

Figure 7. Polar data for the interval 1640 to 1710 UT on 12 March 2001, continuing the format of Figures 5 and 2. The two orange circles show the electron tails detailed in Figure 8. The vertical dotted lines mark excursions into the center of the magnetopause current layer.

Some electron tails appear to be associated with ion events while others are not. Some of the "associated" events occur at the beginnings and others at the ends of accelerated ion intervals. Some of this variability reflects relative motion between Polar and current layer, while other events appear to be temporal changes. We return to this in section 5. We have used minimum variance analyses to look for normal components of the magnetic

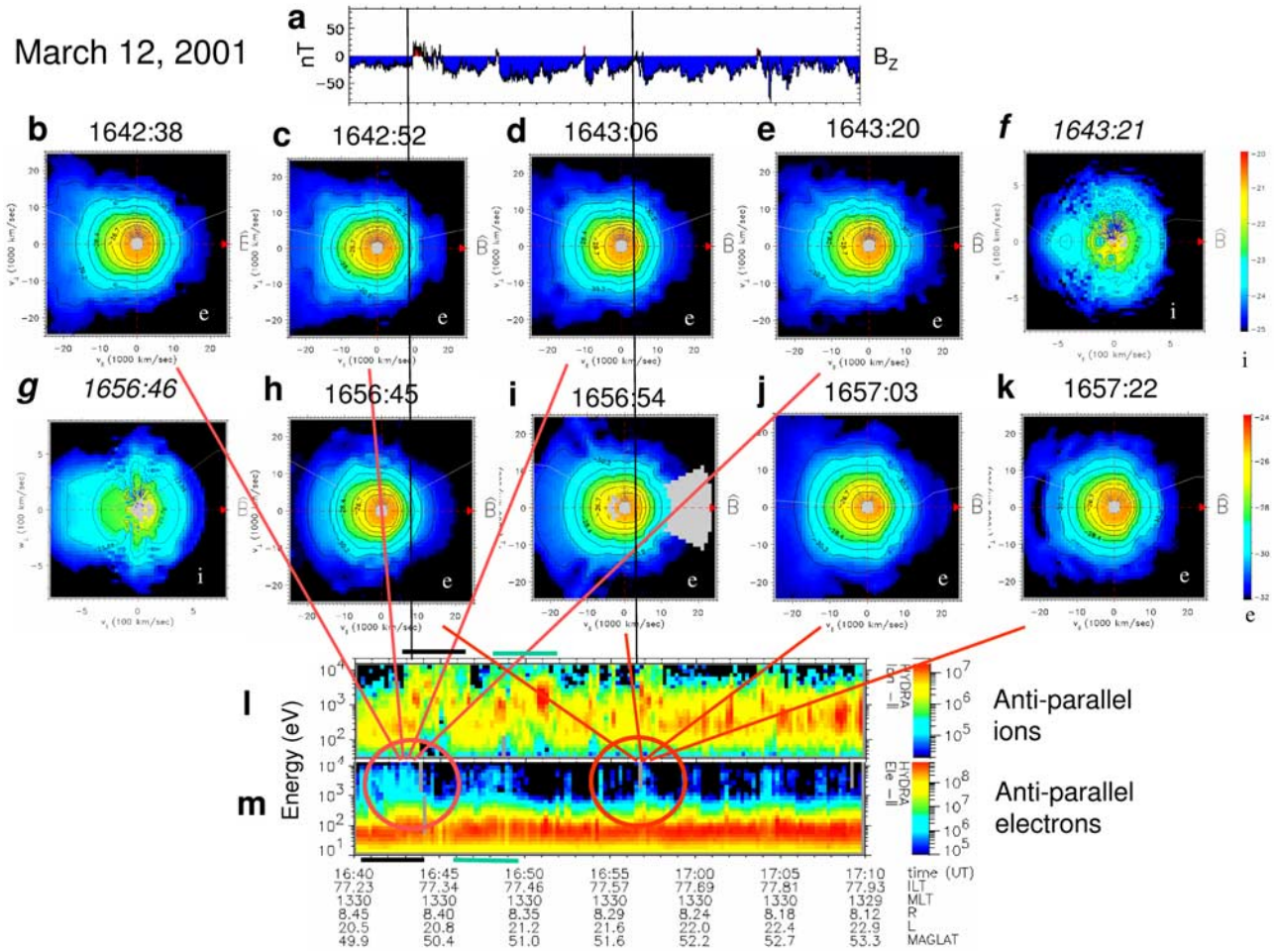

Figure 8. Outer separatrix encounters on 12 March 2001 in a format similar to Figure 6. (b–e and h–k) Electron distribution plots highlighting electron tails in the region of the circles in Figure 9 and keyed to the spectrograms by the colored lines. (f and g) Ion distribution plots at the times of the vertical black lines which are significant to the discussion of the electrons (see text). The black and green bars highlight a suggested correspondence between the data sets, which is explored further in Figure 9 and section 5.

field within the current layers but found none that had statistical significance. However, in some instances the minimum variance analysis indicated that the normal component was of the same order as $|B|$, suggesting that Alfvén waves were propagating along the main field direction.

5. Discussion

[35] Section 4 considers Polar particle and field measurements near the dayside magnetopause at supracusp and subcusp latitudes when the IMF ranged from almost purely southward to having a significant B_Y component. These Polar observations of electron tail events in close spatial/temporal proximity to field-aligned ion and Poynting fluxes confirm present understanding of the magnetopause interactions encapsulated in the model of *Gosling et al.* [1990]. Electron tails were indeed found near the open-closed boundary (inner separatrix) and the open IMF boundary (outer separatrix) associated with active merging sites. For IMF clock angles near 180°, the simple 2-D picture predicts the merging geometry and the relative locations of electron and ion beams near inner and outer separatrices. When the IMF has a significant B_Y component, the structure of the magnetopause becomes more complex involving separated sources. Electron tails can still be used to identify the presence of active remote merging sites on the conjugate magnetopause.

[36] In the following, we comment on the sources of separatrix electrons(section 5.1), consider causal connections between electron tails and 557.7 nm emission episodes in the dayside cusp (section 5.2), and explore some implications for a complex 3-D magnetopause structure when IMF B_Y is large (section 5.3).

5.1. Electron Sources

[37] As electrons, originally the trapped in the plasma sheet, penetrate deep into the diffusion region, gyrotropy breaks down to enable collisionless magnetic merging to proceed [*Vasyliunas*, 1975; *Scudder et al.*, 2002; *Kuznetsova et al.*, 2001]. Within the diffusion region electrons are no longer tied to specific magnetic field lines. Usually, the flow directions of fluid elements in merging geometries are drawn as following the ion centers of mass. If the center-of-mass

crosses the separatrix away from the separator, electrons needed for quasi-neutral flow may not remain collocated with the ions. High electron mobility allows some of them to sample the vicinity of the separator several times, while ions lumber along inertial-dominated trajectories.

[38] Electrons observed along the separatrix were thus demagnetized while near the separator line. Interactions occurring near the separator are the space-time events that lead to time of flight and spatially dispersed sheets of electrons. The highest-energy particles become nested outside those with lower energies. In leaving the diffusion region electrons again become guiding center ordered, reattaching to newly merged field lines at random pitch angles. Other processes such as parallel electric fields encountered during most recent exits from the separator region may add to signatures observed in the separatrix layer. The first field lines that electrons encounter at the edge of the diffusion region define the separatrices. Thus high-energy electron fluxes entering the separator region perpendicular to **B** may exit it with a strong field-aligned component of velocity. Figures 6b and 6c provide clear examples of this reorganization. In that particular case the separation between the electron and ion boundaries, observed as Polar crossed the current layer, was primarily a spatial effect. Plasma sheet electron fluxes, perpendicular to **B**, extend to the highest measurable energies (Figure 6b) and are attached to closed field lines that are about to merged with the IMF. No fluxes parallel to **B** were observed at the highest energies. Figure 6c shows both antiparallel and parallel fluxes at the highest energies. All magnetosheath electrons observed six minutes later had lower energies. We conclude that the high-energy parallel electrons either originated as trapped plasma sheet electrons, or experienced additional acceleration during merging. Since the field-aligned suprathermal electron tails are not present on both side of the magnetopause current layer, some process is necessary to create/rearrange these fluxes. The merging picture described above provides a credible explanation of the observational data.

[39] The suprathermal electrons on which we focused have nearly the smallest gyroradii in the plasma. Thus they are more precise surgical indicators of field line topologies than relativistic electrons and/or trapped ions that have been used in the past to define trapping boundary locations near the magnetopause [e.g., *Williams et al.*, 1985]. These electrons provide clear testimony about the topologies of magnetic field lines threading across the magnetopause. In principle, thermal electrons with smaller gyroradii should provide a more surgical precision for identifying field line topologies. However, they appear at all times in Polar measurements taken near the magnetopause. Thus nonrelativistic suprathermal electrons are the best topology mapping species to be used to specify magnetic connectivity between regions. These particles have different, field-aligned pitch angle distributions in the intermediate spatial layers but have phase-space densities comparable to those of the adjacent plasma sheet. Because their gyroradii are small and leakage is unlikely, we view them as the best remote determinants of where guiding center field lines cross the magnetopause.

[40] We interpret the 31 March 2001 event (Figures 2 and 3) primarily as a spatial feature. In each instance Polar sampled the faster, electron tail populations at the outer separatrix outboard of the ion boundary. Since Polar observed electron tails poleward of the cusp where the magnetic field had similar directions on both sides of the separatrix, we conclude that it was well removed from the separator. Data from the 31 March encounters are consistent with spatial structures that moved back and forth across Polar's path. This case-specific conclusion in no way denies that temporal variations of merging rates can contribute to the relative locations of electron/ion beams. *Fuselier et al.* [1997] also concluded for their predominantly northward IMF cases that the detected keV electrons were of magnetospheric origin.

[41] At a given distance from the merging site, convection carries ions further from the separatrices than higher-velocity tail electrons. Reflecting increased ion travel times, we expect spatial separation between electron and ion boundaries to increase with distance from the merging site. This results in a temporal delay between seeing the electron tails and the corresponding accelerated ions from an active merging site. Wave Poynting flux accompanies the ions away from separator sites. Hence at remote locations, the electron tails become separated from other markers of active merging.

[42] In complex cases, with mixtures of temporal/spatial effects and single-satellite observations, it becomes increasingly difficult to associate particular electron tail events with ion beams propagating from separated merging sites. In the first example shown in Figure 8, Polar was skimming the magnetopause and B_Z was relatively constant as the spacecraft crossed the current layer. The electron tail encounter extended from about 1640 to 1644 UT. From this observation we infer that a similar interval of active merging occurred at a location conjugate to these field lines. The black line over Figure 8l and under Figure 8m highlights this long period of electron tails and the possibly corresponding interval of variable accelerated ions. The transit delay would be about 160 s. Using this delay and an Alfvén speed of 300 km/s we estimate a distance to the merging site to be about 8 R_E. This is commensurate with the distance to the merging site inferred from the simulation result shown in Figure 4e (field lines u and v). Figures 8l and 8m show a second interval of variable electron tails followed by an interval of accelerated ions, highlighted by the green bars.

[43] To further explore possible electron/ion associations, Figure 9 displays the antiparallel ion fluxes shown in Figure 8, but lagged by 160 s with respect to the electron tails. To help maintain perspective on the spatial location of each species relative to the magnetopause current layer, we plotted B_Z twice. Figure 9a shows B_Z as measured at the same time as electrons; Figure 9d shows it lagged with respect to the ions. Red dotted lines, labeled with upper case letters, mark excursions into the center of the current layer in each plot. Heavy dashed black lines denote intervals designated by bars in Figure 8. The deepest excursion into the current layer occurred between lines A and B. In this interval the energy of parallel ions increased significantly, some probably associated with the inner separatrix. Black dotted lines labeled with numbers highlight the beginning of encounters with outer separatrix electron tails. They have an apparent association with

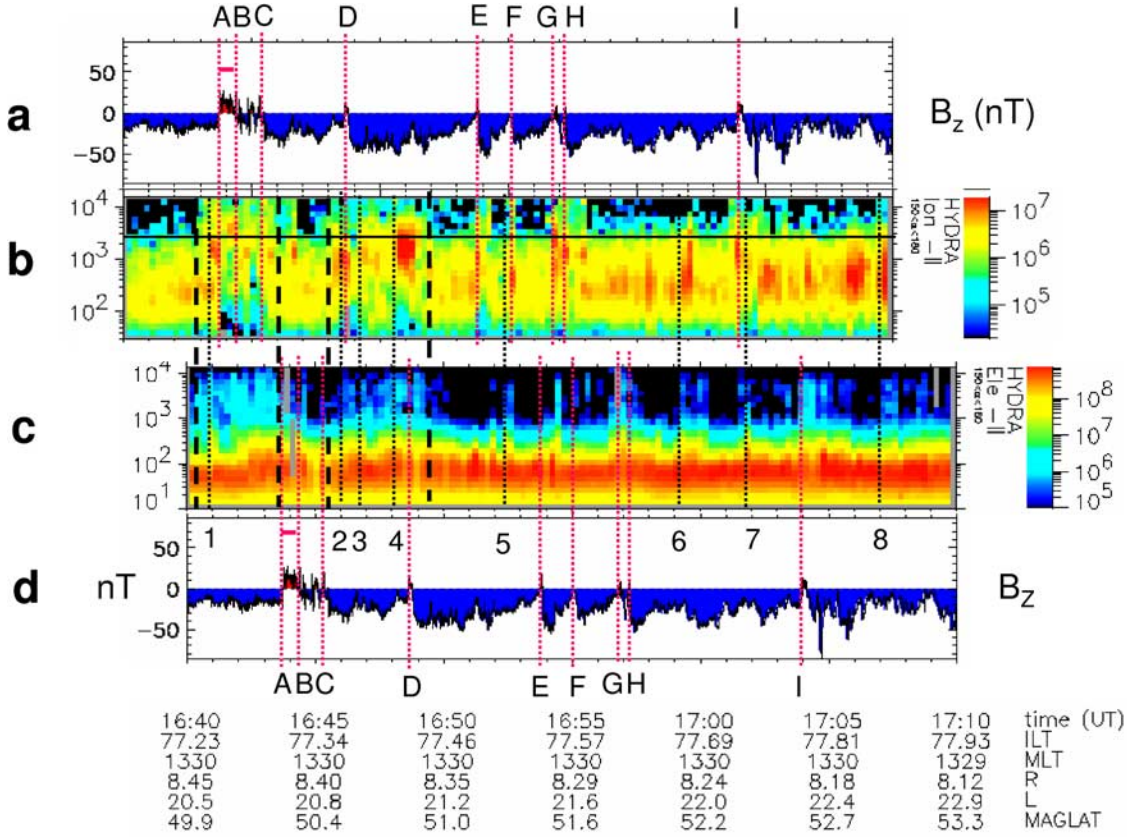

Figure 9. Polar data from Figure 8 with the antiparallel ions lagged by 160 s. The measure B_Z is shown in the time frame of both the electrons and ions to keep in context the spatial location relative to the magnetopause current sheet. Excursions into the center of the current sheet are highlighted by the red dotted lines and labeled with capital letters. Black dotted lines labeled with numbers note times when the electron tails line up with accelerated ions with this lag. The black dashed lines bracket the intervals with the bars in Figure 8. The horizontal line in the ion spectrogram (Figure 9b) has been arbitrarily placed to show the top energy of most of the accelerated ions connected with the outer separatrix (see text).

increases in time-lagged parallel ion fluxes. In selecting these delineations, we have ignored times when excursions into the current layer may have contaminated the correlation with spatial effects. In all cases except line 4, ion fluxes with increased intensities fall near and below the arbitrary horizontal line (at ~3 keV) across the ion spectrogram, suggesting a common origin with electron tails. In general, parallel fluxes observed on the magnetopause side of the current layer tend to have higher energies than nearby parallel ions that we have associate with the outer separatrix. The possibility of dual sources provides a reasonable cause for the discreteness in the accelerated ions.

[44] Electron tails shown in Figures 8h and 8i were observed on the magnetosheath side of the current layer, between excursions into the center of the current sheet, noted by lines G and H in Figure 9. This suggests that the magnetopause was oscillating in a breathing mode. On the basis of the lag suggested by Figure 9, the electron tail in Figures 8h and 8i may belong to ions observed after 1659 UT. Conversely, the electron tail event between lines E and F may be associated with the accelerated ions in Figure 8g. This emphasizes the intricacy of remotely sensing merging in complex geometries associated with IMF B_Y. It is also important to note that because of boundary motions and temporal source variations, there may be cases where accelerated ions are observed without associated electron tails and vice versa.

5.2. Connections to 557.7 nm Emissions

[45] Electron tails observed by Polar near inner separatrices have access to the ionosphere near the boundaries of the dayside cusp with energies sufficient to excite 557.7 nm emissions. Figures 6 and 8 show multiple examples of high-energy (keV) electron tails that Polar encountered for intervals lasting between several tens of seconds and a few minutes. Most examples occurred on the magnetosheath side of the current layer and reflect contacts with outer separatrices attached to active merging sites. However, for every outer separatrix electron tail event there must be a corresponding inner separatrix event, but due to IMF B_Y effects, not necessarily at the same local time. If we interpret these variations as primarily temporal, they define timescales for active merging events. As shown above, complete separation of temporal and spatial effects in the measurements of a single spacecraft is uncertain.

[46] *Maynard et al.* [2004b] interpreted time-varying 557.7 nm emissions observed with all-sky imagers as

"television" pictures of the magnetopause merging process. All-sky images of 557.7 nm emissions uniquely define the temporal histories of particular merging sites. On the basis of the 10-s cadence of 557.7 nm image acquisitions, they concluded that merging occurs simultaneously, but asynchronously, at multiple sites. Active lifetimes of individual sites ranged between 30 s and several minutes. Depending on IMF clock angle θ, merging organized into three regions during the studied $B_Y > 0$ interval. Emissions came from the post-1300 MLT sector while $\theta < 150°$. With still larger clock angles the emissions straddled noon. In the prenoon sector significant 630.0 nm emissions, typically associated with the cusp, were present in the optical records. A DMSP satellite detected fluxes of precipitating electrons with no evidence for a tail population and high cold plasma flows were near the convection reversal of the smaller convection cell. Previously reported ISM simulations show that, under IMF B_Y dominated conditions, the smaller convection cell is driven by merging in the conjugate hemisphere [*Maynard et al.*, 2001a, 2001b].

[47] Since the plasma sheet electrons are trapped and magnetosheath electrons are lower in energy, unless merging is actively proceeding there is no plausible source of field-aligned keV electrons seen by Polar (and needed for 557.7 nm emissions). Similar timescales for 557.7 nm emissions found in all-sky images and electron tail events seen by Polar strongly suggests that both manifest ongoing merging at the magnetopause. This interpretation requires that the electron tail variability observed by Polar was primarily temporal. Relative motions of the boundary and the satellite introduce complicating spatial effects that render definitive time-space separations by a single satellite impossible. However, with multiple satellites and supporting ground-based observations, the electron tails provide a new tool for resolving the temporal/spatial variability in merging.

5.3. Three-Dimensional Magnetopause Structures

[48] The presence of a significant IMF B_Y complicates the geometry of magnetopause dynamics. The locations of Polar during the 12 March interval described above were spatially well removed from expected antiparallel [*Luhmann et al.*, 1984] or component [*Gonzales and Mozer*, 1974] merging sites. The observed negative B_Y component was larger in magnitude than B_Z and was continuous across the magnetopause current layer with a local shear <90°. Note that the IMF clock angle ranged between −120° and −135° during this period. Accelerated ion distributions and electron tails were clearly seen near an inner separatrix (Figures 5i and 5j), and near an outer separatrix (Figures 7i and 7j. These merging signatures were observed at magnetopause locations where the magnetic shear was relatively small. However, simulation results shown in Figure 4 indicate that the magnetic field lines on the inner and outer edges of the magnetopause current layer at Polar's position traced to two very different merging sites on the magnetopause. Because of draping by newly merged magnetic field lines, locally observed magnetic shears bear little relationship to the shear levels at remote merging sites. The magnetopause current layer locally mediates differently directed magnetosheath and magnetospheric magnetic fields. Changes in particle signatures across moderate shear magnetopauses likely reflect remote processes at multiple locations.

6. Conclusions

[49] Field-aligned >0.5 keV electron tails are observed near inner and outer separatrices emanating from active merging sites. These electrons are higher in energy than those in the adjacent magnetosheath. We conclude that they were initially in trapped orbits while on closed field lines within the outer plasma sheet. They should not be observed unless merging is actively proceeding. Because electron velocities are high, they are promptly seen near the separatrices at very large distances from the source merging sites. Hence the presence of these electron tails provides a remote surgical indicator of active merging. Their spatial and temporal structures provide a record of active merging.

[50] Electron tails at the inner separatrix may be bidirectional due to their high speed and low-altitude mirroring off of the ionosphere [e.g., *Ogilvie et al.*, 1984; *Fuselier et al.*, 1995, 1997].

[51] High-energy electron fluxes at outer separatrices are only directed away from merging sites [see also *Fuselier et al.*, 1997]. They are associated with field-aligned Poynting flux and accelerated ions propagating in the same direction.

[52] There is a discernable separation between the electron and ion boundaries as previously reported by *Gosling et al.* [1990]. Because of their higher velocities, electron boundaries remain closer to the separatrices.

[53] When IMF B_Y is present and the magnetic field rotation through the local current layer may be $\ll 180°$. The relationships between merging separators and associated separatrices become more complex. Electron tails and accelerated ions can be found at both inner and outer edges of the magnetopause current layer. However, the sources of these merging signatures at locally low-to-moderate shear magnetopause current layers are interpreted, with the help of ISM simulation results, to be at very different remote locations.

[54] Temporal variability mixed with inherent spatial structuring near the magnetopause, especially in the presence of significant IMF B_Y, complicates the interpretation of electron tail observations. Because of boundary motion and temporal variations of the source, there may be cases where accelerated ions are observed with no associated electron tail and vice versa.

[55] During Polar skimming passes multiple electron tails are observed for intervals lasting for tens of seconds to several minutes. Both temporal and spatial structure may influence the duration and complexity of these encounters.

[56] 557.7 nm images near the dayside cusp boundary indicate that merging can occurring at multiple sites simultaneously, but asynchronously [*Maynard et al.*, 2004b]. The duration at any one site was between 30 s and several minutes. The similar timescales for Polar observing multiple electron tail events are consistent with optical responses seen near the dayside cusp. The similar timescales for 557.7 nm emissions and electron tail encounters indicate that merging is highly time-variable. Since variations observed at Polar mix spatial and temporal effects, care must be exercised in interpreting measurements from a single satellite.

[57] Multiple satellite constellations such as Cluster, in conjunction with ground optical and/or radar observations, offer new opportunities to test our conclusions, thereby establishing the spatial scales of active merging regions, and separating simultaneously present temporal and spatial effects.

[58] **Acknowledgments.** We are grateful to C. W. Smith and D. J. McComas for use of the ACE magnetic field and plasma data. The work at MRC was supported by NASA contract NASW-02017, NASA grant NAG5-3182 (subcontract to the University of California, Berkeley) and the NASA Sun-Earth Connections Theory Program grant NAG5-8135 (subcontract to Boston University). The ISM was developed under sponsorship of the Defense Threat Reduction Agency, 45045 Aviation Drive, Dulles, Virginia. We also acknowledge support from NASA grants and contracts NAG5-2231, NAG5-3328, NAG5-7721, NAG5-7712, NAG5-7883 NAG5-8119, NAS5-30302, NAS5-30316, NASW-99014, NAG5-10883, NAG5-121189, and NAG5-11803 and from AFOSR tasks 2311PL13 and 2311AS.

[59] Lou-Chuang Lee thanks two reviewers for their assistance in evaluating this paper.

References

Cowley, S. W. H. (1982), The causes of convection in the Earth's magnetosphere: A review of developments during the IMS, *Rev. Geophys.*, *20*, 531.

Crooker, N. U. (1979), Dayside merging and cusp geometry, *J. Geophys. Res.*, *84*, 951.

Fuselier, S. A., B. J. Anderson, and T. G. Onsager (1995), Particle signatures of magnetic topology at the magnetopause: AMPTE/CCE observations, *J. Geophys. Res.*, *100*, 11,805.

Fuselier, S. A., B. J. Anderson, and T. G. Onsager (1997), Electron and ion signatures of field line topology at the low-shear magnetopause, *J. Geophys. Res.*, *102*, 4847.

Gonzalez, W. D., and F. S. Mozer (1974), A quantitative model for the potential resulting from reconnection with arbitrary interplanetary magnetic field, *J. Geophys. Res.*, *79*, 4186.

Gosling, J. T., M. F. Thomsen, S. J. Bame, T. G. Onsager, and C. T. Russell (1990), The electron edge of the low latitude boundary layer during accelerated flow events, *Geophys. Res. Lett.*, *17*, 1833.

Hain, K. (1987), The partial donor cell method, *J. Comput. Phys.*, *73*, 131.

Harvey, P., et al. (1995), The electric field instrument on the Polar satellite, *Space Sci. Rev.*, *71*, 583.

Kuznetsova, M. M., M. Hesse, and D. Winske (2001), Collisionless reconnection supported by non-gyrotropic pressure effects in hybrid and particle simulations, *J. Geophys. Res.*, *106*, 3799.

Luhmann, J. G., R. J. Walker, C. T. Russell, N. U. Crooker, J. R. Spreiter, and S. Stahara (1984), Patterns of potential magnetic field merging sites on the dayside magnetopause, *J. Geophys. Res.*, *89*, 1739.

Maynard, N. C. (2003), Svalbard: A window for understanding temporal/spatial aspects of solar wind coupling to the magnetosphere and ionosphere, in *Egeland Symposium on Auroral and Atmospheric Research*, edited by J. Moen and J. A. Holtet, p. 75, Dep. of Phys., Univ. of Oslo, Oslo.

Maynard, N. C. (2005), Coupling the solar-wind/IMF to the ionosphere through the high latitude cusps, *Surv. Geophys.*, *26*, 255.

Maynard, N. C., et al. (2001a), Observation of the magnetospheric "sash" and its implications relative to solar-wind/magnetospheric coupling: A multisatellite event analysis, *J. Geophys. Res.*, *106*, 6097.

Maynard, N. C., et al. (2001b), The response of ionospheric convection to changes in the IMF: Lessons from a MHD simulation, *J. Geophys. Res.*, *106*, 21,429.

Maynard, N. C., W. J. Burke, P. E. Sandholt, J. Moen, D. M. Ober, M. Lester, D. R. Weimer, and A. Egeland (2001c), Observations of simultaneous effects of merging in both hemispheres, *J. Geophys. Res.*, *106*, 24,551.

Maynard, N. C., et al. (2003), Polar, Cluster and SuperDARN evidence for high latitude merging during southward IMF: Temporal/spatial evolution, *Ann. Geophys.*, *21*, 2233.

Maynard, N. C., et al. (2004a), Observed and simulated depletion layers with southward IMF, *Ann. Geophys.*, *22*, 2151.

Maynard, N. C., J. Moen, W. J. Burke, M. Lester, D. M. Ober, J. D. Scudder, K. D. Siebert, D. R. Weimer, C. T. Russell, and A. Balogh (2004b), Temporal/spatial structure of magnetic merging at the magnetopause inferred from 557.7-nm all-sky images, *Ann. Geophys.*, *22*, 2917.

McComas, D. J., S. J. Bame, P. Barber, W. C. Fieldman, J. L. Phillips, and P. Riley (1998), Solar wind electron, proton, and alpha monitor (SWEPAM) on the Advanced Composition Explorer, *Space Sci. Rev.*, *86*, 563.

Ober, D. M., M. F. Thomsen, and N. C. Maynard (2002), Observations of bow shock and magnetopause crossings from geosynchronous orbit on 31 March 2001, *J. Geophys. Res.*, *107*(A8), 1206, doi:10.1029/2001JA000284.

Ogilvie, K. W., R. J. Fitzenreiter, and J. D. Scudder (1984), Observations of electron beams in the low latitude boundary layer, *J. Geophys. Res.*, *89*, 10,723.

Onsager, T. G., J. D. Scudder, M. Lockwood, and C. T. Russell (2001), Reconnection at the high-latitude magnetopause during northward interplanetary magnetic field conditions, *J. Geophys. Res.*, *106*, 25,467.

Russell, C. T., R. C. Snare, J. D. Means, D. Pierce, D. Dearborn, M. Larson, G. Barr, and G. Le (1995), The GGS/Polar magnetic field investigation, *Space Sci. Rev.*, *71*, 563.

Scudder, J. D., K. Ogilvie, and C. T. Russell (1984), The relation of flux transfer events to magnetic reconnection, in *Magnetic Reconnection in Space and Laboratory Plasmas*, *Geophys. Monogr. Ser.*, vol. 30, edited by E. W. Hones Jr., p. 153, AGU, Washington, D. C.

Scudder, J. D., et al. (1995), Hydra: A three dimensional electron and ion instrument for the Polar spacecraft of the GGS mission, *Space Sci. Rev.*, *71*, 459.

Scudder, J. D., F. S. Mozer, N. C. Maynard, and C. T. Russell (2002), Fingerprints of collisionless reconnection at the separator: 1. Ambipolar-Hall signatures, *J. Geophys. Res.*, *107*(A10), 1294, doi:10.1029/2001JA000126.

Siscoe, G., J. Raeder, and A. J. Ridley (2004), Transpolar potential saturation models compared, *J. Geophys. Res.*, *109*, A09203, doi:10.1029/2003JA010318.

Smith, C. W., M. H. Acuna, L. F. Burlaga, J. L'Heureux, N. F. Ness, and J. Scheifele (1998), The ACE Magnetic Field Experiment, *Space Sci. Rev.*, *86*, 613.

Sonnerup, B. U. Ö., G. Paschmann, I. Papamastorakis, N. Sckopke, G. Haerendel, S. J. Bame, J. R. Asbridge, J. T. Gosling, and C. T. Russell (1981), Evidence for magnetic reconnection at the Earth's magnetopause, *J. Geophys. Res.*, *86*, 10,049.

Vasyliunas, V. M. (1975), Theoretical models of magnetic field line merging, *Rev. Geophys.*, *13*, 303.

White, W. W., J. A. Schoendorf, K. D. Siebert, N. C. Maynard, D. R. Weimer, G. L. Wilson, B. U. Sonnerup, G. L. Siscoe, and G. M. Erickson (2001), MHD simulation of magnetospheric transport at the mesoscale, in *Space Weather*, *Geophys. Monogr. Ser.*, vol. 125, edited by P. Song, H. J. Singer, and G. L. Siscoe, p. 229, AGU, Washington, D. C.

Williams, D. J., D. G. Mitchell, T. E. Eastman, and L. A. Frank (1985), Energetic particle observations in the low-latitude boundary layer, *J. Geophys. Res.*, *90*, 5097.

Zwan, B. J., and R. A. Wolf (1976), Depletion of solar wind plasma near a planetary boundary, *J. Geophys. Res.*, *81*, 1636.

W. J. Burke, Air Force Research Laboratory, 29 Randolph Road, Hanscom AFB, MA 01731-3010, USA. (william.burke2@hanscom.af.mil)

M. Lester, Department of Physics and Astronomy, University of Leicester, Leicester LE1 7RH, UK. (mle@ion.le.ac.uk)

N. C. Maynard, Space Science Center, Morse Hall, 39 College Road, University of New Hampshire, Durham, NH 03824, USA. (nelson.maynard@unh.edu)

F. S. Mozer, Space Sciences Laboratory, University of California, 7 Gauss Way, Berkeley, CA 94720-7450, USA. (fmozer@ssl.berkeley.edu)

D. M. Ober, K. D. Siebert, and D. R. Weimer, ATK Mission Research, 589 West Hollis Street, Suite 201, Nashua, NH 03062, USA. (daniel.ober@atk.com; keith.siebert@atk.com; dan.weimer@atk.com)

C. T. Russell, IGPP, University of California, 405 Hilgard Ave., Los Angeles, CA 90095, USA. (ctrussell@igpp.ucla.edu)

N. Sato, National Institute of Polar Research, 1-9-10 Kaga Itabashi-Ku, Tokyo 173, Japan. (nsato@nipr.ac.jp)

J. D. Scudder, Department of Physics and Astronomy, University of Iowa, Van Allen Hall, Iowa City, IA 52242, USA. (jds@space-theory.physics.uiowa.edu)